

Unifying trends found for the $V_N O_{2N-1}$ series by the application of hydrostatic pressure

P. C. Canfield*

*Department of Physics and Solid State Science Center, University of California at Los Angeles,
405 Hilgard Avenue, Los Angeles, California 90024*

J. D. Thompson

Los Alamos National Laboratory, Los Alamos, New Mexico 87545

G. Gruner

*Department of Physics and Solid State Science Center, University of California at Los Angeles,
405 Hilgard Avenue, Los Angeles, California 90024*

(Received 20 September 1989)

The application of hydrostatic pressure to V_7O_{13} , V_8O_{15} , and $(V_{0.98}Cr_{0.02})_8O_{15}$ leads to the formation of pressure-temperature phase diagrams for each of these materials. Analysis of these diagrams allows unifying trends, not apparent at atmospheric pressure, to emerge. Examination of these trends and the nature of the low-temperature antiferromagnetic ground state will be presented.

The $V_N O_{2N-1}$ Magneli series ($N=4-8$) has been of considerable interest for several decades.¹⁻³ The structural similarity of its members and the existence of metal-to-insulator (MI) transitions in most of the series² make it an appealing system for studying the effects of subtle structural changes on phase transitions. But, despite great efforts, the behavior of the members of the series has remained more a catalog of individual properties instead of the hoped for unified behavior anticipated for such a series. In this communication we present the results of an examination of the effects of hydrostatic pressure on V_7O_{13} , V_8O_{15} , and $(V_{0.98}Cr_{0.02})_8O_{15}$, which reveal an overall systematic in the series that is not evident at atmospheric pressure. The earlier, anomalous features, such as the low-temperature metallic ground state of V_7O_{13} ,² are actually part of a larger, general pressure-temperature phase diagram. We also find another manifestation of similarities between members of the series that appear under pressure: a composite phase diagram for the MI transition in V_6O_{11} , V_8O_{15} , and $(V_{0.98}Cr_{0.02})_8O_{15}$.

The $V_N O_{2N-1}$ series is a group of mixed-valence compounds which can be described as having $(N-2)V^{4+}$ ions and $2V^{3+}$ ions per formula unit. The two extremes of this series, V_2O_3 (Ref. 4) and VO_2 (Ref. 5) (corresponding to $N=2$ and $N=\infty$), both undergo MI transitions on cooling. In both cases the transitions are accompanied by lattice distortions and changes in magnetic susceptibility. Whether these changes are driven by the Coulomb correlations, lattice instabilities, or changes in magnetic ground state is still controversial.

The crystal structure of the $V_N O_{2N-1}$ series can be thought of schematically as a derivative of the rutile VO_2 structure,⁶ where the $V_N O_{2N-1}$ structure is simply a rutile block N octahedra in length separated by an oxygen-poor, face-sharing shear plane. Along with this trend in crystal structure, the series members have MI transitions at T_{MI} ,² which generally decrease⁷ to $T_{MI}=0$ at $N=7$ and

start to rise again for $N > 7$. The $N=7$ compound V_7O_{13} remains metallic to 0.5 K, but undergoes an antiferromagnetic (AF) transition at $T_{AF}=45$ K. In V_2O_3 T_{MI} is accompanied by AF ordering,^{2,3} while in VO_2 there is no long-range magnetic order in the insulating state.³ In the Magneli series, anomalies in the magnetic susceptibility associated with AF ordering appear for $T_{AF} < T_{MI}$. Mössbauer measurements on V_4O_7 and V_5O_9 (Refs. 2 and 3) indicate that for $T_{AF} < T < T_{MI}$, there is no long-range magnetic order and the ground state is similar to what is seen in VO_2 . The MI transition in the Magneli series is then one from a paramagnetic metal (PM) to a paramagnetic insulator (PI).

The samples for this study were prepared in a two-step process similar to the method used by Nagasawa, Bando, and Takada.⁸ All measurements of the resistivity were carried out via the four-probe technique, and hydrostatic pressure was applied to the sample by use of a self-clamping pressure cell.⁹

Figure 1(a) shows the resistivity versus temperature curves for V_7O_{13} and V_8O_{15} . The MI transition seen in V_8O_{15} at $T_{MI}=67$ K is typical of the MI transitions seen in other members of the series.² The jump in resistance that is the hallmark of this first-order, MI transition is accompanied by a drop in magnetic susceptibility [Fig. 1(b)] and an increase in unit-cell volume.¹⁰ V_7O_{13} remains metallic to the lowest temperatures; it undergoes a second-order paramagnetic metal (PM) to antiferromagnetic metal (AFM) transition at $T_{AF}=45$ K [note onset of anisotropic magnetic susceptibility seen in Fig. 1(b)]. This PM-AFM transition can be determined resistively by defining T_{AF} as the temperature of the maximum in the logarithmic derivative of $\rho(T)$.^{11,12} Below 7 K, V_7O_{13} has $\rho(T) \propto aT^2$, with $a=0.6 \mu\Omega \text{ cm/K}^2$. Figure 1(b) shows the magnetic susceptibilities of V_7O_{13} and V_8O_{15} ; as can be seen, V_7O_{13} develops an anisotropic susceptibility below T_{AF} . The values of T_{MI} and T_{AF} are equally well determined from resistivity or susceptibility

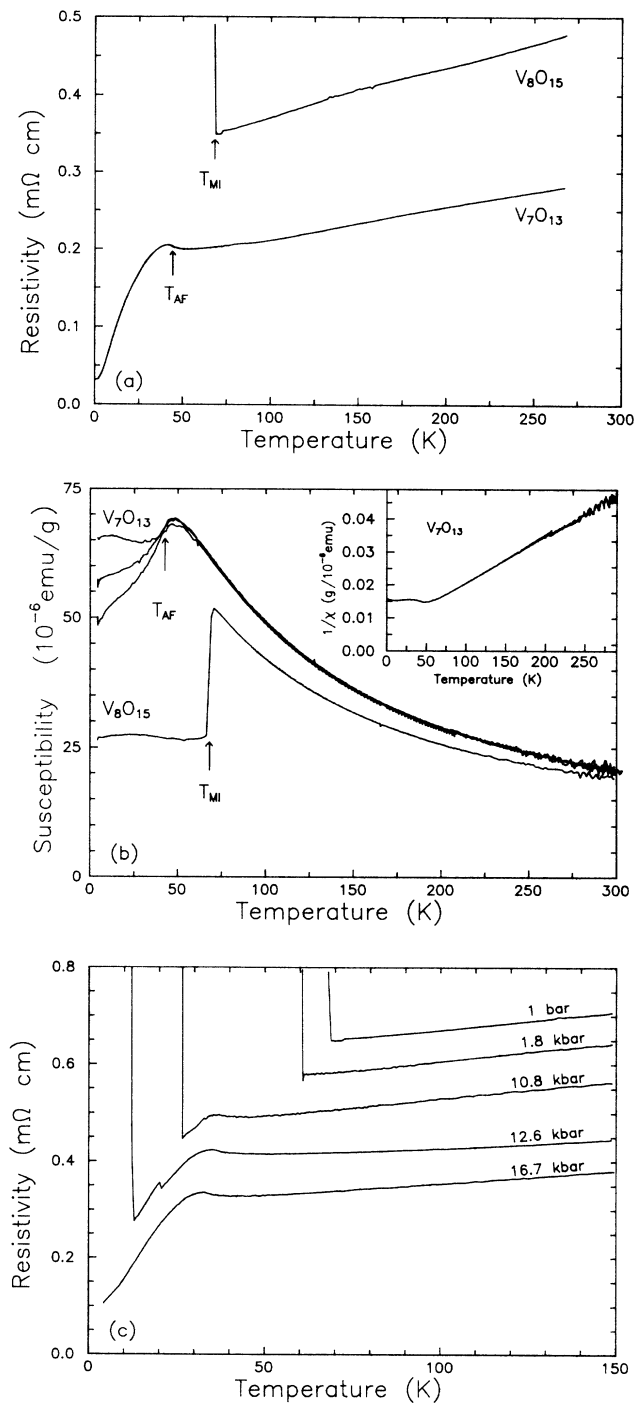


FIG. 1. (a) Electrical resistivity vs temperature for V_7O_{13} and V_8O_{15} samples at atmospheric pressure; (b) magnetic susceptibility of V_7O_{13} and V_8O_{15} at atmospheric pressure. V_7O_{13} data are from a single crystal shown for three mutually perpendicular field orientations with respect to the single crystal. The single crystal has not been oriented with x rays, therefore, the three mutually perpendicular directions are arbitrarily chosen with respect to the triclinic unit cell. The inset shows inverse susceptibility vs temperature for one of the V_7O_{13} data sets. (c) Resistivity vs temperature curves for V_8O_{15} at five representative pressures. Curves are shifted slightly along the y axis for clarity. Note: small jumps in the data seen in the 10.8- and 12.6-kbar plots are experimental artifacts.

measurements. It should be noted that the anisotropy of V_7O_{13} is unusual in that the powder χ is quite high,^{11,13} with the three single-crystal χ 's bunching so closely to it. [Griffing *et al.*¹¹ measured the susceptibility of a polycrystalline sample of V_7O_{13} as being similar to the middle of the three single-crystal measurements shown in Fig. 1(b).] V_8O_{15} shows a large drop in χ at T_{MI} , and remains isotropic throughout the measured temperature range.^{14,15} The inset to Fig. 1(b) shows $1/\chi$ versus temperature for one of the V_7O_{13} data sets. $\chi(T)$ can be fitted by a Curie-Weiss temperature dependence: $\chi(T) = C/(T + \Theta) + \chi_0$ where the Curie constant $C = \mu_{eff}^2/3k_B$, Θ is the Curie temperature, and χ_0 is the temperature-independent susceptibility. For V_7O_{13} , $\mu_{eff} = 2.11\mu_B$ per vanadium site, $\Theta = 38$ K, and $\chi_0 = 0.5 \mu\text{emu/g}$. It is interesting to notice that the effective moment μ_{eff} that would be associated with a purely ionic V_7O_{13} structure, $5(V^{4+})$ and $2(V^{3+})$ per formula unit, is $\mu_{eff} = 2.13\mu_B$ per vanadium site. This nearly ionic susceptibility is also a generic feature of the V_NO_{2N-1} series for $T > T_{MI}$ or $T > T_{AF}$.

Since V_7O_{13} appears to be anomalous in the V_NO_{2N-1} series, we deemed it probable that either V_7O_{13} or its neighbor V_8O_{15} (having the lowest T_{MI} in the series at $T_{MI} = 67$ K) may show interesting behavior when placed under hydrostatic pressure. Figure 2(a) is the pressure-temperature phase diagram for V_7O_{13} . Application of pressure simply suppresses T_{AF} in a linear manner with a slope of -0.75 K/kbar. The extrapolated pressure at which $T_{AF}(P) = 0$ is $P \approx 70$ kbar.

Figure 1(c) shows ρ vs T plots for V_8O_{15} at five representative pressures. Initially, application of pressure simply suppresses T_{MI} , as seen in other members of the series,¹⁶ and ultimately, for pressures greater than 13 kbar, T_{MI} is fully suppressed. Since the jump in the resistivity is quite discontinuous, even at 12 kbar, the MI transition is probably still a first-order phase transition. But lacking either x-ray or specific-heat measurements under pressure, this assumption should be noted.

The surprising feature of V_8O_{15} under pressure is that, for pressures greater than 9 kbar, a resistive anomaly identical to that seen in V_7O_{13} appears as T_{MI} is suppressed through this more slowly decreasing transition. Due to (i) the qualitative similarities of the ρ vs T plots of V_7O_{13} and high-pressure V_8O_{15} , and (ii) the fact that V_7O_{13} and V_8O_{15} are so structurally similar, we tentatively identify the transition seen in V_8O_{15} under high pressures as a PM-AFM transition.

Figure 2(b) is the pressure-temperature phase diagram for V_8O_{15} . As in V_7O_{13} , T_{AF} drops with a slope of -0.75 K/kbar. In the range of pressures $9 < P < 13$ kbar there is a series of transitions PM-AFM-PI. This may be the first observation of such a series of transitions as a function of temperature, specifically, the loss of long-range magnetic order on going from an AFM to a PI state.

In V_2O_3 the addition of small amounts of Cr can be thought of as an application of negative, "chemical" pressure.⁴ In order to further examine the pressure dependence of the V_8O_{15} phase diagram, a sample of nominally 2% Cr-doped V_8O_{15} was prepared. Figure 2(c) is the pressure-temperature phase diagram for $(V_{0.98}Cr_{0.02})_8O_{15}$. As seen in V_8O_{15} under high pressures, there is a

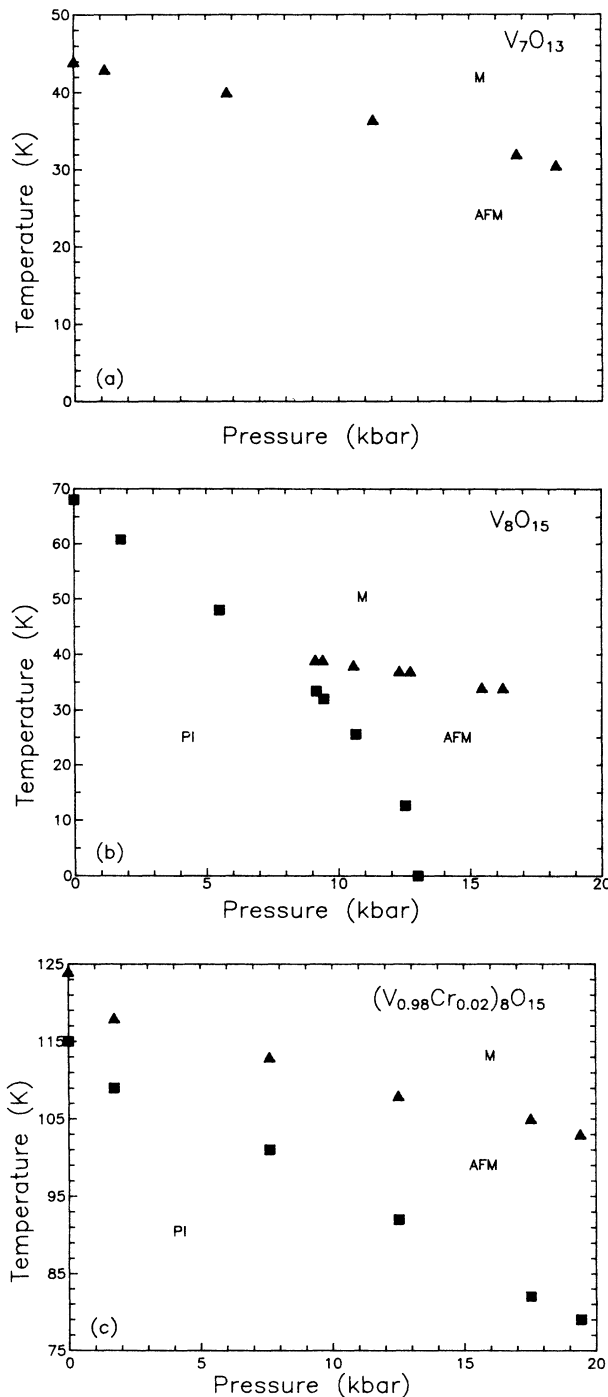


FIG. 2. (a) Pressure-temperature phase diagram for V_7O_{13} . (b) Pressure-temperature phase diagram for V_8O_{15} . (c) Pressure-temperature phase diagram for $(V_{0.98}Cr_{0.02})_8O_{15}$.

series of transitions, PM-AFM-PI. Both the MI and PM-AFM transitions have been shifted due to the addition of the Cr, but the phase diagram is fundamentally similar to that for pure V_8O_{15} . The rate of suppression of T_{AF} is again -0.75 K/kbar, and T_{MI} falls at a greater rate, so that the two transitions separate as pressure is increased.

By examining the phase diagrams for these three ma-

terials it becomes clear that the PM-AFM transition seen in V_7O_{13} at atmospheric pressure is not anomalous. The PM-AFM transition clearly appears in V_8O_{15} at pressures above 9 kbar and in $(V_{0.98}Cr_{0.02})_8O_{15}$ at all pressures. In all cases this magnetic transition has the same pressure dependence: -0.75 K/kbar. It is possible that other members of the V_NO_{2N-1} series will have this transition as part of their high-pressure phase diagrams, although none of them show it up to an applied pressure of 20 kbar.¹⁶

The nature of the low-temperature metallic state is intriguing. V_7O_{13} has an electronic specific heat¹¹ of 40 mJ/K²molV and has $\rho(T) \propto T^2$ for $T < 7$ K. Both of these measurements are consistent with a narrow band of correlated electrons. While there is an AF transition at $T_{AF} = 45$ K (for atmospheric pressure), it is unlikely that all of the moments involved in the high-temperature Curie tail, $\mu_{eff} = 2.11\mu_B$ per vanadium site, are ordering. This is indicated by the fact that the change in entropy, ΔS , through the transition is less than 10% of what would be expected for the loss of spin degrees of freedom for a fully ionic crystal.¹¹ The possibility of only a fraction of the moments ordering is also borne out by the curious nature of the anisotropic χ in Fig. 1(b). Not only is the $\Delta\chi(T=0)$ small for the three mutually perpendicular orientations, but the fact that the powder susceptibility is so high^{11,13} indicates that there exists a large paramagnetic moment that is not involved in the AF ordering. There are initial indications from neutron scattering¹⁷ that the static susceptibility (for $T > T_{AF}$) derives, at least in part, from ferromagnetic correlations in the conduction band. A rough estimate of the magnitude of the ordered moment, based on the specific heat and magnetic susceptibility measurements, would be $1\mu_B$ /formula unit.

Another feature that is apparent from the phase diagrams is that T_{AF} and T_{MI} have different pressure dependencies. While T_{AF} drops linearly in all three diagrams, T_{MI} drops at a much faster rate. In both V_8O_{15} and $(V_{0.98}Cr_{0.02})_8O_{15}$ the pressure dependence is closer to quadratic than linear, with T_{MI} dropping the fastest in the pure V_8O_{15} . By looking solely at the pressure dependence of the MI transition in V_8O_{15} , $(V_{0.98}Cr_{0.02})_8O_{15}$, and V_6O_{11} (Ref. 16) we find another unifying feature: by shifting the pressure scale for V_6O_{11} and $(V_{0.98}Cr_{0.02})_8O_{15}$ so as to allow the matching of $T_{MI}(P)$, we find a composite phase diagram for the MI transition (Fig. 3). The shifts in pressure relative to pure V_8O_{15} are -20 kbar for $(V_{0.98}Cr_{0.02})_8O_{15}$ (this is the negative chemical pressure mentioned earlier⁴), and -40 kbar for V_6O_{11} . While V_4O_7 can also be included as part of this even- N phase diagram,¹⁶ the shift in pressure in that case would be more arbitrary,¹⁸ since applied pressures of up to 20 kbar fail to suppress the MI transition sufficiently to allow an overlap of $T_{MI}(P)$ with V_6O_{11} .

The existence of this unified pressure- T_{MI} phase diagram for V_6O_{11} , $(V_{0.98}Cr_{0.02})_8O_{15}$, and V_8O_{15} is precisely the behavior that has been sought in the V_NO_{2N-1} series. While ongoing single-crystal x-ray measurements of the crystal structure of V_6O_{11} and V_8O_{15} (Ref. 11) both above and below T_{MI} will hopefully shed some light on whether the N dependence of T_{MI} can be correlated to any

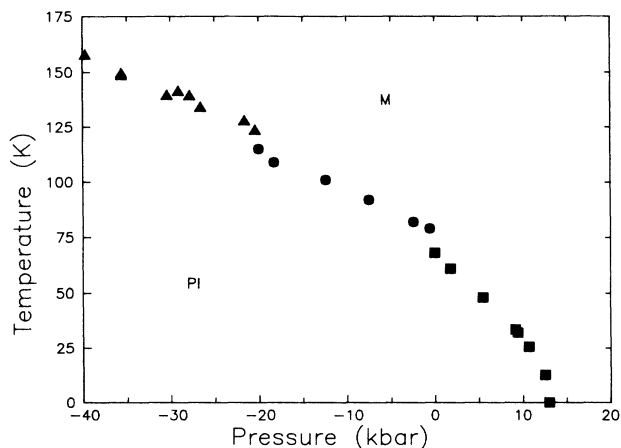


FIG. 3. Composite pressure-MI temperature phase diagram for V_6O_{11} , $(V_{0.98}Cr_{0.02})_8O_{15}$, and V_8O_{15} . Squares are unshifted V_8O_{15} data, circles are $(V_{0.98}Cr_{0.02})_8O_{15}$ data shifted by -20 kbar, and triangles are V_6O_{11} data shifted by -40 kbar.

structural features, it will probably be the structural analysis of these materials under hydrostatic pressure that will reveal what structural parameters, if any, effect $T_{MI}(P, N)$.

In summary, the long sought after unifying behavior of the V_NO_{2N-1} series starts to appear when hydrostatic pressure is applied. The previous, apparently anomalous, low-temperature metallic ground state of V_7O_{13} appears

in both V_8O_{15} and $(V_{0.98}Cr_{0.02})_8O_{15}$ when appropriate pressures are applied, and the pressure dependence of T_{AF} is the same, -0.75 K/kbar, in all three materials. The nature of this low-temperature metallic ground state is still somewhat unclear, but analysis of the anisotropic magnetic susceptibility, and the change in entropy at T_{AF} indicate only a partial ordering of moments, $1-2\mu_B$ /formula unit, and the remaining isotropic susceptibility at low temperature, the large electronic specific heat, and the low-temperature resistivity point to a narrow, correlated band existing in the ground state. The application of pressure also allows the formation of a composite phase diagram for T_{MI} . The pressure dependence of T_{MI} for V_6O_{11} , $(V_{0.98}Cr_{0.02})_8O_{15}$, and V_8O_{15} can be united into a single phase diagram by simply shifting the relative pressure scales so as to allow the overlap of $T_{MI}(P)$ for each material. While these initial results are encouraging, an overall picture of the N and pressure dependencies of T_{MI} , as well as a clear model of either the low-temperature metallic or insulating ground states, are still lacking.¹⁹

We would like to thank G. Mihaly and W. Beyermann for many helpful discussions, J. Cooper for his help in building the magnetometer used in these measurements, and B. Alavi for his help in preparing the samples. Work at Los Alamos was performed under the auspices of the U.S. Department of Energy, and work at the University of California at Los Angeles was supported by National Science Foundation Grant No. DMR 8620340.

*Present address: Los Alamos National Laboratory, Mail Stop K764, Los Alamos, NM 87545.

¹G. Andersson, *Acta Chem. Scand.* **8**, 1599 (1954); S. Andersson and L. Jahnberg, *Arkiv Kemi* **21**, 43 (1963).

²S. Kachi, K. Kosuge, and H. Okinaka, *J. Solid State Chem.* **6**, 258 (1973).

³S. Kachi, *J. Phys. Chem. Solids* **28**, 1613 (1967).

⁴N. F. Mott, *Metal Insulator Transitions* (Taylor and Francis, London, 1974); D. McWhan and J. Remeika, *Phys. Rev. B* **2**, 3734 (1970); J. M. Honig, *J. Solid State Chem.* **45**, 1 (1982).

⁵N. Mott, *Metal Insulator Transitions* (Ref. 4); M. Marezio, D. McWhan, J. Remeika, and P. Dernier, *Phys. Rev. B* **5**, 2541 (1971).

⁶H. Megaw, *Crystal Structures: A Working Approach* (Saunders, Philadelphia, 1973).

⁷There is actually an even- N , odd- N variation in T_{MI} with the odd- N members ($N=5,7$) having lower T_{MI} 's than the extrapolated values from the even- N data.

⁸K. Nagasawa, Y. Bando, and T. Takada, *J. Cryst. Growth* **17**, 143 (1972).

⁹J. D. Thompson, *Rev. Sci. Instrum.* **55**, 231 (1984).

¹⁰P. C. Canfield, S. Khan, and C. Strouse (unpublished); M. Marezio, D. B. McWhan, P. D. Dernier, and J. P. Remeika, *J. Solid State Chem.* **6**, 419 (1973); M. Marezio, P. D. Dernier, D. B. McWhan, and S. Kachi, *ibid.* **11**, 301 (1974).

¹¹B. Griffling, S. Shivashankar, S. Nagata, S. Faile, and J.

Honig, *Phys. Rev. B* **25**, 1703 (1982).

¹²S. Alexander, J. Helman, and I. Balberg, *Phys. Rev. B* **13**, 304 (1976).

¹³S. Nagata, B. F. Griffing, G. D. Khattak, and P. H. Keesom, *J. Appl. Phys.* **50**, 7575 (1979).

¹⁴S. Nagata, P. H. Keesom, and S. P. Faile, *Phys. Rev. B* **20**, 2886 (1979); see an anomalous hysteresis in χ vs T for $T < 7$ K in V_8O_{15} . This can be associated with the AF transition but is still poorly understood.

¹⁵Although Mössbauer measurements have not been performed on V_8O_{15} for $T_{AF} < T < T_{MI}$, the similarity in both crystal structure and low-temperature dimerization pattern with V_4O_7 and V_5O_9 makes the designation of this ground state as a paramagnetic insulator (PI) reasonable.

¹⁶P. C. Canfield, J. D. Thompson, and G. Gruner, *Physica B* (to be published).

¹⁷F. Mezei *et al.* (unpublished).

¹⁸ V_4O_7 data can be incorporated into Fig. 3 by shifting it roughly -100 kbar with respect to V_8O_{15} .

¹⁹There has been some recent theoretical work done on the MI transition seen in Cr-doped V_2O_3 by J. Spalek, A. Datta, and J. M. Honig [*Phys. Rev. B* **33**, 4891 (1986); *Phys. Rev. Lett.* **59**, 728 (1987)], but the application of this model to either VO_2 or the Magneli series is difficult due to the large lattice distortions caused by the MI transition in these materials.